Approach to solving spin-boson dynamics via non-Markovian quantum trajectories

Zeng-Zhao Li,[1,2] Cho-Tung Yip,[2] Hai-Yao Deng,[2,3] Mi Chen,[1,4] Ting Yu,[1,5] J. Q. You,[1,6,*] and Chi-Hang Lam[2,*]

[1]*Beijing Computational Science Research Center, Beijing 100084, China*

[2]*Department of Applied Physics, Hong Kong Polytechnic University, Hung Hom, Hong Kong, China*

[3]*International Center for Materials Nanoarchitechtonics, National Institute for Materials Science, Namiki 1-1, Tsukuba 305-0044, Japan*

[4]*Department of Physics, Fudan University, Shanghai 200433, China*

[5]*Center for Controlled Quantum Systems and Department of Physics and Engineering Physics, Stevens Institute of Technology, Hoboken, New Jersey 07030, USA*

[6]*Synergetic Innovation Center of Quantum Information and Quantum Physics, University of Science and Technology of China, Hefei, Anhui 230026, China*

(Received 12 June 2014; published 26 August 2014)

We develop a systematic and efficient approach for numerically solving the non-Markovian quantum state diffusion equation for an open quantum system that can be strongly coupled to an environment. As an important application, we consider a real-time simulation of a spin-boson model in a strong-coupling regime that is difficult to deal with using conventional methods. We show that the non-Markovian stochastic Schrödinger equation can be efficiently implemented as a real-time simulation for this model, so as to give an accurate description of spin-boson dynamics beyond the rotating-wave approximation.

DOI: 10.1103/PhysRevA.90.022122 PACS number(s): 03.65.Yz, 42.50.Lc

I. INTRODUCTION

The dynamics of open quantum systems has been extensively studied in the last decades due to its pivotal importance in the areas of quantum optics, quantum dissipative dynamics, and quantum information [1–3]. The Lindblad master equations under the Born-Markov approximations are the major theoretical tools in depicting quantum evolution under the influence of external noises, but they are doomed to fail when the system-environment coupling becomes strong or when the environment is a structured medium [4]. Moreover, the widely used rotating-wave approximation (RWA) ceases to be valid at a strong-coupling regime [1,5–7]. It becomes clear that to correctly explain the novel quantum-mechanical phenomena arising from the strong-coupling physics, the counter-rotating terms neglected in the RWA must be taken into account properly. In addition, the counter-rotating terms are known to be important in understanding quantum Zeno and anti-Zeno effects [8–10]. All the current researches going beyond the RWA and Markov approximation have shown the necessity of developing a powerful approach to dealing with new physics arising from the strong coupling between the open quantum system of interest and its environment [9–13].

A stochastic Schrödinger equation, named the non-Markovian quantum state diffusion (QSD) equation, derived from a microscopic model has several advantages over the exact master equations. While the exact master equations exist only for a few solvable models (see, e.g., Ref. [14]), the exact QSD equation has been established for a generic class of quantum open systems [15]. However, the applications of the exact QSD equation are severely limited unless this time-nonlocal integro-differential equation can be cast into a numerically implementable time-local form [15–18].

In real-world problems, solving the exact dynamical equations in a strong-coupling regime is very difficult. Therefore it is imperative to develop an efficient perturbative method that can be implemented to solve open system dynamics dictated by the strong coupling and structured medium.

In this paper, we develop a systematic and efficient approach to solving the non-Markovian QSD equations for open quantum systems up to arbitrary orders of noises. The major breakthrough is to convert the non-Markovian QSD equation into a set of coupled stochastic ordinary differential equations (SODEs) which efficiently evaluates a series expansion of the previously unsolvable O operator up to arbitrarily high orders. The method can be generally applied to an arbitrary finite-state open system coupled to a bosonic bath with a Lorentzian noise spectrum at zero temperature. As an important example, our method is used to solve a spin-boson model with a Lorentzian environment at zero temperature in the strong-coupling regime that is previously intractable when real-time quantum dynamics is needed.

II. EXACT QSD EQUATION

To put our discussion into perspective, we first consider a generic open quantum system with the following Hamiltonian (setting $\hbar = 1$)[15]:

$$H_{\rm tot} = H_{\rm sys} + \sum_k (g_k L b_k^\dagger + g_k^* L^\dagger b_k) + \sum_k \omega_k b_k^\dagger b_k, \qquad (1)$$

where $H_{\rm sys}$ is the Hamiltonian of the system under consideration, L is the Lindblad operator, and b_k denotes the annihilation operator of the kth mode of the bosonic bath. The state of the bath may be specified by a set of complex numbers $\{z_k\}$ labeling the (Bargmann) coherent states of all modes. The function z_t that characterizes time-dependent states of the bath may be defined by the Fourier expansion $z_t^* \equiv -i \sum_k g_k^* z_k^* e^{i\omega_k t}$. When z_k is interpreted as a Gaussian random variable, then z_t becomes a Gaussian process with

*Corresponding authors: jqyou@csrc.ac.cn; C.H.Lam@polyu.edu.hk

the correlation function obtained by the statistical mean $\alpha(t-s)=\langle z_t z_s^*\rangle=\sum_k |g_k|^2 e^{-i\omega_k(t-s)}$. For the simple case with a zero-temperature bath, the system state at time t obtained from projecting the total state to the bath state $|z\rangle$, $\psi_t(z^*)\equiv\langle z|\Psi_{\rm tot}(t)\rangle$, which is called a quantum trajectory, obeys a linear QSD equation [15],

$$\dot{\psi}_t=-iH_{\rm sys}\psi_t+Lz_t^*\psi_t-L^\dagger\bar{O}\psi_t. \tag{2}$$

Here, the O operator is defined by $\delta\psi_t/\delta z_s^*=O(t,s,z^*)\psi_t$, and $\bar{O}(t,z^*)=\int_0^t\alpha(t-s)O(t,s,z^*)ds$. Evaluating the O operator poses a major challenge in solving quantum open systems in real-world applications. It is remarkable that the evolution is completely decoupled from projections to other bath states and hence can be solved independently. In practice, one may adopt an important sampling scheme in which the normalized system state $\tilde{\psi}_t(\tilde{z}^*)=\psi_t(\tilde{z}^*)/|\psi_t(\tilde{z}^*)|$ is governed by the norm-conserving nonlinear QSD equation [15],

$$\begin{aligned}\dot{\tilde{\psi}}_t=&-iH_{\rm sys}\tilde{\psi}_t+(L-\langle L\rangle_t)\tilde{z}_t^*\tilde{\psi}_t\\&-[(L^\dagger-\langle L^\dagger\rangle_t)\bar{O}-\langle(L^\dagger-\langle L^\dagger\rangle_t)\bar{O}\rangle_t]\tilde{\psi}_t,\end{aligned} \tag{3}$$

where $\bar{O}$ denotes $\bar{O}(t,\tilde{z}^*)$ and $\langle\ldots\rangle_t=\langle\tilde{\psi}_t|\ldots|\tilde{\psi}_t\rangle$. We define a shifted noise as $\tilde{z}_t^*=z_t^*+y_t$, where the shift $y_t=\int_0^t\alpha^*(t-s)\langle L^\dagger\rangle_s ds$ satisfies $y_0=0$, and

$$\dot{y}_t=-\gamma y_t+\alpha^*(0)\langle L^\dagger\rangle_t. \tag{4}$$

The state of the open quantum system at t, represented by the reduced density matrix $\rho_t={\rm Tr}_{\rm env}|\Psi_{\rm tot}\rangle\langle\Psi_{\rm tot}|$, can be recovered from an ensemble average $\rho_t=\langle|\tilde{\psi}_t(\tilde{z}^*)\rangle\langle\tilde{\psi}_t(\tilde{z}^*)|\rangle$.

The QSD equations (2) and (3) are exact. A key challenge is the determination of the O operator contained in these equations. For most practical problems except for a few specific examples where the exact O may be explicitly determined [15–18], one has to resort to a functional expansion [16] in terms of $\tilde{z}_t^*$, which after adapting to $\bar{O}$ is written as

$$\begin{aligned}\bar{O}(t,\tilde{z}^*)=&\,\bar{O}^{(0)}(t)+\int_0^t\bar{O}^{(1)}(t,\upsilon_1)\tilde{z}_{\upsilon_1}^*d\upsilon_1\\&+\int_0^t\int_0^t\bar{O}^{(2)}(t,\upsilon_1,\upsilon_2)\tilde{z}_{\upsilon_1}^*\tilde{z}_{\upsilon_2}^*d\upsilon_1d\upsilon_2+\cdots\\&+\int_0^t\cdots\int_0^t\bar{O}^{(n)}(t,\upsilon_1,\cdots,\upsilon_n)\tilde{z}_{\upsilon_1}^*\cdots\tilde{z}_{\upsilon_n}^*\\&\times d\upsilon_1\cdots d\upsilon_n+\cdots,\end{aligned} \tag{5}$$

where $\bar{O}^{(n)}$ is symmetric with respect to the time variables υ_i. However, finding $\bar{O}^{(n)}$ and performing the integrations for higher-order terms are formidable tasks and have only been performed up to $n\leqslant 2$ for some specific models [19].

III. SODE FORMULATION

In this work, we show that the QSD perturbation may be carried out to an arbitrary order of noise terms. Specifically, we can efficiently evaluate Eq. (5) up to $\mathcal{N}=100$ perturbative terms for the spin-boson model under consideration. We first rewrite it as

$$\bar{O}(t,\tilde{z}^*)=\sum_{n=0}^{N_Q}Q_0^{(n)}(t,\tilde{z}^*), \tag{6}$$

where $N_Q=\mathcal{N}$ nominally but we allow $N_Q<\mathcal{N}$ when higher-order terms are vanishingly small. We also define a generalized operator,

$$\begin{aligned}Q_m^{(n)}(t,\tilde{z}^*)=&\int_0^t\cdots\int_0^t\alpha(t-\upsilon_1)\cdots\alpha(t-\upsilon_m)\tilde{z}_{\upsilon_{m+1}}^*\cdots\\&\times\tilde{z}_{\upsilon_n}^*\bar{O}^{(n)}(t,\upsilon_1,\ldots,\upsilon_n)d\upsilon_1\cdots d\upsilon_n.\end{aligned} \tag{7}$$

For $m\neq 0$, $Q_m^{(n)}$ does not contribute directly to $\bar{O}$ but is an auxiliary operator which needs to be solved simultaneously. Let $\langle g_k\rangle$ be a mean coupling strength. Up to leading orders $\alpha(t)\sim\langle g_k\rangle^2$, we have $\tilde{z}_t^*\sim\langle g_k\rangle$, and hence $Q_m^{(n)}\sim\langle g_k\rangle^{n+m+2}$ when using also $\bar{O}^{(n)}\sim\alpha(t)$ [16].

From Eq. (7), each $Q_m^{(n)}$ is an n-dimensional definite time integral from 0 to t in every dimension. At time $t=0$, $Q_m^{(n)}$ is exactly zero. For sufficiently small t, $Q_m^{(n)}$ roughly scales as t^n, assuming that the integrand varies smoothly with t; then $Q_m^{(n)}\sim t^n\to 0$ for large n and small t. Therefore the infinite series in Eq. (5), which involves only the $Q_0^{(n)}$'s in particular, is then guaranteed to be convergent at least for small t. More generally, $Q_m^{(n)}$ has a finite support (i.e., a domain where $Q_m^{(n)}$ takes nonzero values) on the (n,m) plane, which expands with t. Therefore Eq. (5) and equivalently Eq. (6) can be arbitrarily accurate at a finite N_Q. As t increases, especially for a strong-coupling regime, the support might expand unboundedly. In practice, we impose the constraint $N_Q\leqslant\mathcal{N}$ by choosing a large $\mathcal{N}$ to assure the accuracy, and consider $Q_m^{(n)}$ only up to $n+m\leqslant\mathcal{N}$, corresponding to order $\langle g_k\rangle^{\mathcal{N}+2}$.

For simplicity, we consider the environmental noise z_t characterized by the Ornstein-Uhlenbeck noise with the autocorrelation

$$\alpha(t-s)=\frac{\Gamma\gamma}{2}e^{-\gamma|t-s|}. \tag{8}$$

Taking the time derivative of Eq. (7) and applying the evolution equation of $\bar{O}^{(n)}$ [16], we arrive at our central analytical result after some algebra (see Appendix A):

$$\begin{aligned}\dot{Q}_m^{(n)}=&\,\delta_{n,0}\alpha(0)L+\frac{m}{n'}\alpha(0)\big[L,Q_{m-1}^{(n-1)}\big]\\&+\frac{n-m}{n'}\tilde{z}_t^*\big[L,Q_m^{(n-1)}\big]\\&-(m+1)\gamma Q_m^{(n)}-i\big[H_{\rm s},Q_m^{(n)}\big]\\&-\sum_{k=0}^{n}\sum_{l=l_a}^{l_b}\frac{C_l^kC_{n-m-l}^{n-k}}{C_m^n}\big[L^\dagger Q_{k-l}^{(k)},Q_{m-k+l}^{(n-k)}\big]\\&-(n+1)L^\dagger Q_{m+1}^{(n+1)},\end{aligned} \tag{9}$$

where $n'=\max\{1,n\}$, $l_a=\max\{0,k-m\}$, $l_b=\min\{k,n-m\}$, $Q_m^{(-1)}=Q_{-1}^{(n)}=0$, and C_l^k is the binomial coefficient. Equations (3), (4), and (9) for $n+m\leqslant\mathcal{N}$ then constitute a set of coupled SODEs from which $\tilde{\psi}_t(\tilde{z}^*)$ can be obtained. To make the results more apparent, we also explicitly show in Appendix B some examples of the evolution equations for the lower-order terms $Q_m^{(n)}(t,\tilde{z}^*)$.

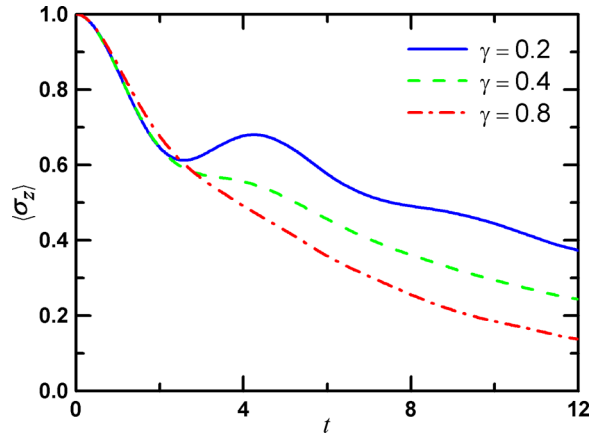

FIG. 1. (Color online) Spin state $\langle\sigma_z\rangle$ for various memory parameters: $\gamma = 0.2$, 0.4, and 0.8. Here $\omega = 1$, $\Gamma\gamma = 0.2$, and $\mathcal{N} = 100$.

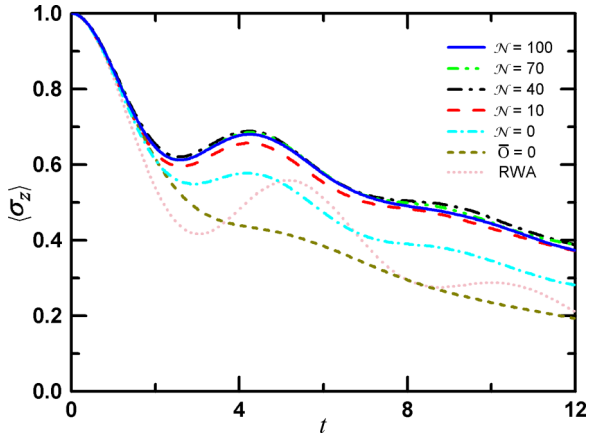

FIG. 2. (Color online) Spin state $\langle\sigma_z\rangle$ for $\mathcal{N} = 100$, 70, 40, 10, and 0, $\tilde{O} = 0$, and RWA. Here $\gamma = 0.2$ and $\Gamma\gamma = 0.2$.

IV. RESULTS ON A SPIN-BOSON MODEL

Now we apply our method to a spin-boson model with $H_{\rm sys} = \frac{\omega}{2}\sigma_z$ and $L = \sigma_x$ [20–23], assuming an initial system state of $\langle\sigma_z\rangle = 1$ with the bath at zero temperature. In the following calculations, all coupling strengths and frequencies are in units of ω. We use $\sqrt{\Gamma\gamma/2}$ to characterize the coupling strength between the system and the environment. This is consistent with the single-mode case where the bath spectrum function (i.e., the Lorentzian form) for the Ornstein-Uhlenbeck noise is reduced to $J(\omega) = \Gamma\gamma\delta(\omega)/2$, with $\Gamma\gamma/2$ being the square of the usual single-mode coupling constant. We take $\Gamma\gamma = 0.2$ in order to consider the strong-coupling regime [24] (i.e., $\sqrt{\Gamma\gamma/2} \sim 0.32 \in [0.1, 1]$ in units of ω) and $\gamma = 0.2$, 0.4, and 0.8 for the bath memory time $1/\gamma$ to show Markovian and non-Markovian behaviors. Each statistical mean involves an ensemble of $N_z = 8000$ of complex colored Gaussian noise z_t obeying the correlation function in Eq. (8). For each realization z_t, we obtain one quantum trajectory $\tilde{\psi}_t(\tilde{z}_t^*)$ by numerically solving the SODEs up to $\mathcal{N} = 100$ terms. The reduced density matrix of the system is recovered by a statistical mean: $\rho_t = \langle|\tilde{\psi}_t(\tilde{z}^*)\rangle\langle\tilde{\psi}_t(\tilde{z}^*)|\rangle$.

Figure 1 shows the evolutions of $\langle\sigma_z\rangle$. For $\gamma = 0.2$ corresponding to a relatively long memory time in our study, an oscillatory behavior superimposed with a nonexponential decay of $\langle\sigma_z\rangle$ is observed, exemplifying strong non-Markovian effects. The decay behavior becomes more monotonic as γ is increased. At $\gamma = 0.8$, it is essentially exponential early on, demonstrating weak memory effects [20]. In general, exponential decay is ensured when $t \gg 1/\gamma$. Because the ground state of the total system is no longer a product of the unexcited system state and the vacuum state of the reservoir when including the counter-rotating terms, collapse and revival of the system's state population occur, which indicates that $\langle\sigma_z\rangle$ approaches zero instead of -1 for a long time. As will be explained below, $\langle\sigma_z\rangle$ reported in Fig. 1 admits about 1% error.

For comparison, the result for the most interesting case of $\gamma = 0.2$ is replotted in Fig. 2 and labeled as $\mathcal{N} = 100$. The results for other values of $\mathcal{N}$ are also shown. We also plot $\langle\sigma_z\rangle$ calculated similarly using RWA by taking $L = \sigma_-$. RWA is known to be accurate when the system-bath coupling is weak. At the strong coupling considered here, we observe that the non-Markovian oscillatory behavior of $\langle\sigma_z\rangle$ is successfully reproduced. However, in the RWA, $\langle\sigma_z\rangle$ drops considerably faster due to neglecting the counter-rotating terms.

V. ALGORITHMS AND ACCURACY

Figure 3(a) plots the average $\langle\parallel Q_0^{(n)} \parallel\rangle = \langle{\rm Tr}\sqrt{Q_0^{(n)\dagger} Q_0^{(n)}}\rangle$ of the trace norm of each perturbative term in Eq. (6) for $\gamma = 0.2$. Initial oscillatory behaviors are observed in the four lowest orders and should be responsible for the similar oscillations in $\langle\sigma_z\rangle$. Moreover, note that the low-order terms rise from 0 earlier than the high-order ones. This verifies that the support of $Q_m^{(n)}$ expands gradually from low orders as explained above. For $n \gtrsim 10$, $\langle\parallel Q_0^{(n)} \parallel\rangle$ is already close to 0, implying good convergence of the functional expansion. We also observe that $\langle\parallel Q_0^{(n)} \parallel\rangle$ tends to become constant at large t. Such saturation is indeed clearly observed for $\gamma = 0.4$ and 0.8 at $t \gg 1/\gamma$, and the saturated value decreases exponentially to 0 with n. For any given realization, $\parallel Q_0^{(n)} \parallel$, however, persists to fluctuate and arrives only at a dynamic steady state.

To solve the SODEs efficiently, we hence put $N_Q = 1$ initially and increase it adaptively during the time integration with Euler's method and a time step $\Delta t = 0.02$. Only $Q_m^{(n)}$ values for $n + m \leqslant N_Q$ are calculated and the rest are approximated by zeros. $Q_m^{(n)}$ values for $n + m = N_Q$ are monitored at every time step. If the magnitude of any of their matrix elements goes beyond a threshold $\epsilon_{\rm thres} = 10^{-8}$, N_Q is incremented unless it has reached $\mathcal{N}$, and the last Euler's step is recalculated.

The number of calculated terms N_Q hence indicates the number of nonzero terms in the functional expansion. It depends on both t and z_t^*, and hence admits ensemble fluctuations. Figure 3(b) plots the probability density $P(N_Q)$ of its final value at $t = 12$ for $N_Q < \mathcal{N}$ from the simulations in Fig. 1. Interestingly, we observe that the distribution is not narrow. The tails fit very well to exponential forms. The average $\langle N_Q\rangle$ increases with the memory time $1/\gamma$. Moreover, it also increases with the coupling constant $\Gamma\gamma$ (results not shown).

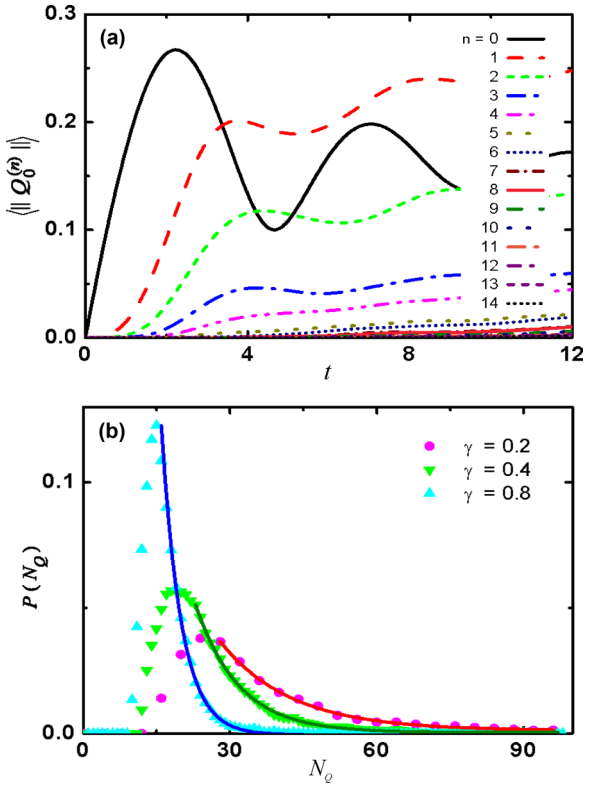

FIG. 3. (Color online) (a) Average $\langle\| Q_0^{(n)} \|\rangle$ of the trace norm of perturbative terms $Q_0^{(n)}$ from the simulation in Fig. 1 for $\gamma = 0.2$. (b) The probability density $P(N_Q)$ of N_Q at $t = 12$ from the simulations in Fig. 1 for $\gamma = 0.2$, 0.4, and 0.8. Solid lines show fits to exponential distributions for the tails of the distributions.

To study the importance of individual terms, we have also simulated with $\bar{O} = 0$ (i.e., $\mathcal{N} < 0$), $\mathcal{N} = 0$, and $\mathcal{N} = 10$. The results are shown in Fig. 2. We observe, as expected, that the decay of $\langle\sigma_z\rangle$ becomes faster and more monotonic when fewer terms are included. Incidentally, the results for $\bar{O} = 0$ and $\mathcal{N} = 0$ for $\gamma = 0.2$ in Fig. 2 resemble the accurate results for $\gamma = 0.8$ and 0.4, respectively, in Fig. 1. This suggests that neglecting the non-Markovian terms effectively decreases the bath correlation time. For $\mathcal{N} = 10$, $\langle\sigma_z\rangle$ has nearly converged to the accurate result at $\mathcal{N} = 100$.

Moreover, for $\gamma = 0.2$ and $\mathcal{N} \gtrsim 20$, the solution of the SODEs unexpectedly becomes nontrivial. Once N_Q is constrained at $\mathcal{N}$ and the magnitude of a matrix element of $Q_m^{(n)}$ with $n + m = \mathcal{N}$ exceeds a tolerance $\epsilon_{\rm tol} = 10^{-4}$, the SODEs eventually become unstable with $Q_m^{(n)}$ at large n and m, diverging smoothly but rapidly with t even at much reduced Δt. The concerned noise realization z_t^* is hence rejected and excluded from all ensemble averages. Allowing rejection, we have also performed simulations at $\mathcal{N} = 40$ and 70 and the results are plotted in Fig. 2. The rejection rates for $\mathcal{N} = 40, 70$, and 100 are $R = 11\%$, 6.6%, and 5.4%, respectively. Due to the exponential distribution of N_Q, R is expected to decrease exponentially against $\mathcal{N}$. We find that the rejected noise realizations z_t^* in general are those with large magnitudes. The rejection induces errors associated with an ensemble bias which decreases with $\mathcal{N}$. Again, the result for $\mathcal{N} = 70$ has nearly converged to our most accurate result at $\mathcal{N} = 100$. For $\gamma = 0.4$ and 0.8, as shown in Fig. 1, $\langle N_Q\rangle$ is much smaller and thus noise rejection events become rare.

Since the SODEs are exact, the errors occurring in our algorithm can be fully analyzed. The rms error of $\langle\sigma_z\rangle$ can be approximated by $\sqrt{\mathcal{E}_{N_z}^2 + \mathcal{E}_{\Delta t}^2 + \mathcal{E}_{\mathcal{N}}^2}$. Here, $\mathcal{E}_{N_z} \sim 1/\sqrt{N_z}$ denotes the ensemble sampling error. For all calculations reported in Fig. 1, we find $\mathcal{E}_{N_z} \simeq 0.004$ after averaging over time. The time discretization error $\mathcal{E}_{\Delta t}$ is found to be about 0.001 from simulations with identical noise but different Δt. Also, $\mathcal{E}_{\mathcal{N}}$ is due to including at most $\mathcal{N} = 100$ perturbative terms. For $\gamma = 0.4$ and 0.8, $\mathcal{E}_{\mathcal{N}} \simeq 0$ because higher-order terms are vanishingly small. For $\gamma = 0.2$, we find $\mathcal{E}_{\mathcal{N}} \simeq 0.002$ from comparing results at $\mathcal{N} = 70$ and 100 with identical noise. Finally, $\langle\sigma_z\rangle$ admits about 1% error in all three cases. The simulations for $\gamma = 0.2$, 0.4, and 0.8 take about 36, 10, and 2 days, respectively, to execute on an Intel core-i7 CPU core. Indeed, QSD approaches are fully capable of parallelization. The accuracy for $\gamma = 0.4$ and 0.8 can be further improved substantially by increasing N_z. More challenging is the $\gamma = 0.2$ case, since one must also reduce $\mathcal{E}_{\mathcal{N}}$ by increasing $\mathcal{N}$. This leads to much more intensive computations. Note that the program run time is of the order $N_z\mathcal{N}^4/\Delta t$. Minimizing $\mathcal{E}_{\mathcal{N}}$ and $\mathcal{E}_{N_z}$ simultaneously to produce accurate results will be critical and challenging when pushing to even stronger couplings.

VI. CONCLUSION

In conclusion, we have developed a high-order non-Markovian QSD approach for open quantum systems based on a set of coupled SODEs which can be efficiently implemented in numerical simulations. As an important example, our method is applied to a spin-boson model with a Lorentzian bath spectrum at zero temperature in the strong-coupling regime. Note that a generalization to the finite temperature case is straightforward [25]. In particular, for this spin-boson model, the finite-temperature non-Markovian QSD equation actually takes the exact same form as the zero-temperature QSD equation. An extension to general interaction spectra may also be possible by including coupled equations for a full set of new operators analogous to $Q_m^{(n)}$ in Eq. (7), each with a particular subset of α's replaced by their derivatives. Our numerical simulations of the spin-boson model have shed a new light on the spin dynamics without the RWA. It is shown that even though the RWA may successfully reproduce non-Markovian spin-state transient oscillations, it cannot accurately capture the bath memory effects. We emphasize that our proposed approach is efficient and readily applicable to numerically solving the non-Markovian quantum dynamics for open quantum systems with strong coupling and structured bosonic medium. Possible further applications include, for example, multilevel quantum systems in a strong-coupling regime [26], photonic band-gap materials [4,27], and also chemical and biological systems [28].

Note added: Recently, we become aware of a different kind of numerically exact hierarchical equations by Strunz and coworkers [29].

ACKNOWLEDGMENTS

Z.Z.L and C.T.Y contributed equally to this work. This work is supported by the National Natural Science Foundation of China (Grant No. 91121015), the National Basic Research

Program of China (Grant No. 2014CB921401), the NSAF (Grant No. U1330201), Hong Kong GRF (Grant No. 501213), HK PolyU (Grant No. G-YM41), and the China Postdoctoral Science Foundation (Grant No. 2012M520146). T.Y. is grateful to Prof. J. Q. You for the hospitality during his visit to the CSRC, Beijing.

APPENDIX A: DERIVATION OF EQ. (9)

In this section we provide basic ideas and key derivations to support our central analytical result given by Eq. (9). Our motivation for a systematic and efficient approach to solving the non-Markovian quantum state diffusion equation is to solve the formidable challenge in the numerical evaluation of the multidimensional integrals in the functional expansion of the O operator [16],

$$O(t,s,\tilde{z}^*) = O^{(0)}(t,s) + \int_0^t O^{(1)}(t,s,\upsilon_1)\tilde{z}^*_{\upsilon_1}d\upsilon_1 + \int_0^t\int_0^t O^{(2)}(t,s,\upsilon_1,\upsilon_2)\tilde{z}^*_{\upsilon_1}\tilde{z}^*_{\upsilon_2}d\upsilon_1 d\upsilon_2 + \cdots + \int_0^t\cdots\int_0^t O^{(n)}(t,s,\upsilon_1,\ldots,\upsilon_n)\tilde{z}^*_{\upsilon_1}\cdots\tilde{z}^*_{\upsilon_n}d\upsilon_1\cdots d\upsilon_n + \cdots, \tag{A1}$$

or the $\bar{O}$ operator in Eq. (5) of the main text. In the notation of Eq. (6) of the main text, it is clear that only the value of $Q_0^{(n)}$ contributes to $\bar{O}$ directly. However, in order to have a closed set of equations, we need to introduce more general operators $Q_m^{(n)}$ with $n \geqslant m \geqslant 0$, which are defined in Eq. (7) with $\bar{O}^{(n)} = \int_0^t \alpha(t-s)O^{(n)}ds$. To derive readily solvable evolution equations, we differentiate $Q_m^{(n)}$ with respect to time. The calculation is in general straightforward, except that one of the terms contains in the integrand a nontrivial factor $\int_0^t \alpha(t-s)\dot{O}^{(n)}(t,s,\upsilon_1,\ldots,\upsilon_n)ds$. Using an expression of $\dot{O}^{(n)}$ from Ref. [16], we obtain

$$\begin{aligned}\int_0^t \alpha(t-s)\dot{O}^{(n)}(t,s,\upsilon_1,\ldots,\upsilon_n)ds &= -i[H_S,\bar{O}^{(n)}(t,\upsilon_1,\ldots,\upsilon_n)] \\ &\quad - \frac{1}{n!}\sum_{P_n\in S_n}\sum_{k=0}^{n}[L^\dagger\bar{O}^{(k)}(t,\upsilon_{P_n(1)},\ldots,\upsilon_{P_n(k)}),\bar{O}^{(n-k)}(t,\upsilon_{P_n(k+1)},\ldots,\upsilon_{P_n(n)})] \\ &\quad - (n+1)L^\dagger\int_0^t \alpha(t-\upsilon_{n+1})\bar{O}^{(n+1)}(t,\upsilon_1,\ldots,\upsilon_n,\upsilon_{n+1})d\upsilon_{n+1}.\end{aligned} \tag{A2}$$

In the following we consider cases $n = 0$ and $n > 0$ separately for the Ornstein-Uhlenbeck noise in Eq. (8). For $n = 0$, Eq. (7) reduces to

$$Q_0^{(0)}(t,\tilde{z}^*) = \bar{O}^{(0)}(t). \tag{A3}$$

Differentiating Eq. (A3) gives

$$\dot{Q}_0^{(0)}(t,\tilde{z}^*) = \alpha(0)L - \gamma Q_0^{(0)}(t,\tilde{z}^*) - i\big[H_S,Q_0^{(0)}(t,\tilde{z}^*)\big] - \big[L^\dagger Q_0^{(0)}(t,\tilde{z}^*),Q_0^{(0)}(t,\tilde{z}^*)\big] - L^\dagger Q_0^{(1)}(t,\tilde{z}^*), \tag{A4}$$

where we have used Eq. (A2) with $n = 0$ and the initial condition $O^{(0)}(t,t) = L$ [16].

For $n > 0$, we differentiate Eq. (7) and obtain

$$\begin{aligned}\dot{Q}_m^{(n)}(t,\tilde{z}^*) &= \partial_t Q_m^{(n)}(t,\tilde{z}^*) \\ &= \big(\partial_{t_1}+\partial_{t_2}+\partial_{t_3}+\partial_{t_4}+\partial_{t_5}\big)\int_0^{t_1}ds\int_0^{t_2}d\upsilon_1\cdots\int_0^{t_2}d\upsilon_m\int_0^{t_3}d\upsilon_{m+1}\cdots\int_0^{t_3}d\upsilon_n\alpha(t_4-s) \\ &\quad\times\alpha(t_4-\upsilon_1)\cdots\alpha(t_4-\upsilon_m)\tilde{z}^*_{\upsilon_{m+1}}\cdots\tilde{z}^*_{\upsilon_n}O^{(n)}(t_5,s,\upsilon_1,\ldots,\upsilon_n)|_{t_1=t_2=t_3=t_4=t_5=t} \\ &= \frac{m}{n}\alpha(0)\big[L,Q_{m-1}^{(n-1)}(t,\tilde{z}^*)\big] + \frac{n-m}{n}\tilde{z}_t^*\big[L,Q_m^{(n-1)}(t,\tilde{z}^*)\big] - (m+1)\gamma Q_m^{(n)}(t,\tilde{z}^*) - i\big[H_s,Q_m^{(n)}(t,\tilde{z}^*)\big] \\ &\quad - \sum_{k=0}^{n}\sum_{l=l_a}^{l_b}\frac{C_l^k C_{n-m-l}^{n-k}}{C_m^n}\big[L^\dagger Q_{k-l}^{(k)}(t,\tilde{z}^*),Q_{m-k+l}^{(n-k)}(t,\tilde{z}^*)\big] - (n+1)L^\dagger Q_{m+1}^{(n+1)}(t,\tilde{z}^*).\end{aligned} \tag{A5}$$

Here we have used Eq. (A2), the symmetric property of $\bar{O}$ with regard to time variables υ_i, i.e.,

$$\bar{O}^{(n)}(t,\upsilon_1,\ldots,\upsilon_i,\ldots,\upsilon_j,\ldots,\upsilon_n) = \bar{O}^{(n)}(t,\upsilon_1,\ldots,\upsilon_j,\ldots,\upsilon_i,\ldots,\upsilon_n), \tag{A6}$$

and the conditions [16]

$$O^{(n)}(t,t,\upsilon_1,\ldots,\upsilon_n)=0 \quad (\text{for } n\geq 1), \tag{A7}$$

$$O^{(n)}(t,s,t,\upsilon_2,\ldots,\upsilon_n)=\frac{1}{n}[L,O^{(n-1)}(t,s,\upsilon_2,\ldots,\upsilon_n)] \quad (\text{for } n\geq 1). \tag{A8}$$

Equations (A4) and (A5) can be combined and rewritten as Eq. (9) of the main text.

APPENDIX B: EXAMPLES OF $\dot{Q}_m^{(n)}$ AT LOW ORDERS

In this section, we give some examples of the evolution equations for the lower-order terms $Q_m^{(n)}(t,\tilde{z}^*)$ in order to make our results more apparent.

(1) When $n=1,m=0$,

$$\begin{aligned}\dot{Q}_0^{(1)}(t,\tilde{z}^*)&=\tilde{z}_t^*\big[L,Q_0^{(0)}(t,\tilde{z}^*)\big]-\gamma Q_0^{(1)}(t,\tilde{z}^*)-i\big[H_{\rm s},Q_0^{(1)}(t,\tilde{z}^*)\big]\\&\quad-\sum_{k=0}^{1}\sum_{l=\max\{0,k\}}^{\min\{k,1\}}\frac{C_l^kC_{1-l}^{1-k}}{C_0^1}\big[L^\dagger Q_{k-l}^{(k)}(t,\tilde{z}^*),Q_{-k+l}^{(1-k)}(t,\tilde{z}^*)\big]-2L^\dagger Q_1^{(2)}(t,\tilde{z}^*)\\&=\tilde{z}_t^*\big[L,Q_0^{(0)}(t,\tilde{z}^*)\big]-\gamma Q_0^{(1)}(t,\tilde{z}^*)-i\big[H_{\rm s},Q_0^{(1)}(t,\tilde{z}^*)\big]-\big[L^\dagger Q_0^{(0)}(t,\tilde{z}^*),Q_0^{(1)}(t,\tilde{z}^*)\big]\\&\quad-\big[L^\dagger Q_0^{(1)}(t,\tilde{z}^*),Q_0^{(0)}(t,\tilde{z}^*)\big]-2L^\dagger Q_1^{(2)}(t,\tilde{z}^*).\end{aligned} \tag{B1}$$

(2) When $n=m=1$,

$$\begin{aligned}\dot{Q}_1^{(1)}(t,\tilde{z}^*)&=\alpha(0)\big[L,Q_0^{(0)}(t)\big]-2\gamma Q_1^{(1)}(t,\tilde{z}^*)-i\big[H_{\rm s},Q_1^{(1)}(t,\tilde{z}^*)\big]\\&\quad-\sum_{k=0}^{1}\sum_{l=\max\{0,k-1\}}^{\min\{k,0\}}\frac{C_l^kC_{0-l}^{1-k}}{C_1^1}\big[L^\dagger Q_{k-l}^{(k)}(t,\tilde{z}^*),Q_{1-k+l}^{(1-k)}(t,\tilde{z}^*)\big]-2L^\dagger Q_2^{(2)}(t,\tilde{z}^*)\\&=\alpha(0)\big[L,Q_0^{(0)}(t)\big]-2\gamma Q_1^{(1)}(t,\tilde{z}^*)-i\big[H_{\rm s},Q_1^{(1)}(t,\tilde{z}^*)\big]-\big[L^\dagger Q_0^{(0)}(t,\tilde{z}^*),Q_1^{(1)}(t,\tilde{z}^*)\big]\\&\quad-\big[L^\dagger Q_1^{(1)}(t,\tilde{z}^*),Q_0^{(0)}(t,\tilde{z}^*)\big]-2L^\dagger Q_2^{(2)}(t,\tilde{z}^*).\end{aligned} \tag{B2}$$

(3) When $n=2,m=1$,

$$\dot{Q}_1^{(2)}(t,\tilde{z}^*)=\frac{\alpha(0)}{2}\big[L,Q_0^{(1)}(t,\tilde{z}^*)\big]+\frac{\tilde{z}_t^*}{2}\big[L,Q_1^{(1)}(t,\tilde{z}^*)\big]-2\gamma Q_1^{(2)}(t,\tilde{z}^*)-i\big[H_{\rm s},Q_1^{(2)}(t,\tilde{z}^*)\big]-\left\{\sum_{k=0}^{2}\mathcal{E}_k\right\}-3L^\dagger Q_2^{(3)}(t,\tilde{z}^*),$$

where

$$\begin{aligned}\left\{\sum_{k=0}^{2}\mathcal{E}_k\right\}&=\frac{1}{2!}\int_0^t d\upsilon_1\int_0^t d\upsilon_2\alpha(t-\upsilon_1)\tilde{z}_{\upsilon_2}^*\sum_{P_2\in S_2}\sum_{k=0}^{2}[L^\dagger\bar{O}^{(k)}(t,\upsilon_{P_2(1)},\ldots,\upsilon_{P_2(k)}),\bar{O}^{(2-k)}(t,\upsilon_{P_2(k+1)},\ldots,\upsilon_{P_2(2)})]\\&=\frac{1}{2!}\int_0^t d\upsilon_1\int_0^t d\upsilon_2\alpha(t-\upsilon_1)\tilde{z}_{\upsilon_2}^*\{2[L^\dagger\bar{O}^{(0)}(t),\bar{O}^{(2)}(t,\upsilon_1,\upsilon_2)]+[L^\dagger\bar{O}^{(1)}(t,\upsilon_1),\bar{O}^{(1)}(t,\upsilon_2)]\\&\quad+[L^\dagger\bar{O}^{(1)}(t,\upsilon_2),\bar{O}^{(1)}(t,\upsilon_1)]+2[L^\dagger\bar{O}^{(2)}(t,\upsilon_1,\upsilon_2),\bar{O}^{(0)}(t)]\}\\&=\sum_{k=0}^{2}\sum_{l=\max\{0,k-1\}}^{\min\{k,1\}}\frac{C_l^kC_{1-l}^{2-k}}{C_1^2}\big[L^\dagger Q_{k-l}^{(k)}(t,\tilde{z}^*),Q_{1-k+l}^{(2-k)}(t,\tilde{z}^*)\big].\end{aligned} \tag{B3}$$

Therefore,

$$\begin{aligned}\dot{Q}_1^{(2)}(t,\tilde{z}^*)&=\frac{\alpha(0)}{2}\big[L,Q_0^{(1)}(t,\tilde{z}^*)\big]+\frac{\tilde{z}_t^*}{2}\big[L,Q_1^{(1)}(t,\tilde{z}^*)\big]-2\gamma Q_1^{(2)}(t,\tilde{z}^*)-i\big[H_{\rm s},Q_1^{(2)}(t,\tilde{z}^*)\big]-3L^\dagger Q_2^{(3)}(t,\tilde{z}^*)\\&\quad-\frac{1}{2}\big\{2\big[L^\dagger Q_0^{(0)}(t,\tilde{z}^*),Q_1^{(2)}(t,\tilde{z}^*)\big]+\big[L^\dagger Q_1^{(1)}(t,\tilde{z}^*),Q_0^{(1)}(t,\tilde{z}^*)\big]+\big[L^\dagger Q_0^{(1)}(t,\tilde{z}^*),Q_1^{(1)}(t,\tilde{z}^*)\big]\\&\quad+2\big[L^\dagger Q_1^{(2)}(t,\tilde{z}^*),Q_0^{(0)}(t,\tilde{z}^*)\big]\big\}.\end{aligned} \tag{B4}$$

(4) When $n = m = 2$,

$$\begin{aligned}\dot{Q}_2^{(2)}(t,\tilde{z}^*) &= \alpha(0)\big[L, Q_1^{(1)}(t,\tilde{z}^*)\big] - 3\gamma Q_2^{(2)}(t,\tilde{z}^*) - i\big[H_s, Q_2^{(2)}(t,\tilde{z}^*)\big] \\ &\quad - \sum_{k=0}^{2}\sum_{l=\max\{0,k-2\}}^{\min\{k,0\}} \frac{C_l^k C_{0-l}^{2-k}}{C_2^2}\big[L^\dagger Q_{k-l}^{(k)}(t,\tilde{z}^*), Q_{2-k+l}^{(2-k)}(t,\tilde{z}^*)\big] - 3L^\dagger Q_3^{(3)}(t,\tilde{z}^*) \\ &= \alpha(0)\big[L, Q_1^{(1)}(t,\tilde{z}^*)\big] - 3\gamma Q_2^{(2)}(t,\tilde{z}^*) - i\big[H_s, Q_2^{(2)}(t,\tilde{z}^*)\big] - \big[L^\dagger Q_0^{(0)}(t,\tilde{z}^*), Q_2^{(2)}(t,\tilde{z}^*)\big] \\ &\quad - \big[L^\dagger Q_1^{(1)}(t,\tilde{z}^*), Q_1^{(1)}(t,\tilde{z}^*)\big] - \big[L^\dagger Q_2^{(2)}(t,\tilde{z}^*), Q_0^{(0)}(t,\tilde{z}^*)\big] - 3L^\dagger Q_3^{(3)}(t,\tilde{z}^*). \end{aligned} \tag{B5}$$

(5) When $n = 3, m = 1$,

$$\begin{aligned}\dot{Q}_1^{(3)}(t,\tilde{z}^*) &= \frac{1}{3}\alpha(0)\big[L, Q_0^{(2)}(t,\tilde{z}^*)\big] + \frac{2}{3}z_t\big[L, Q_1^{(2)}(t,\tilde{z}^*)\big] - 2\gamma Q_1^{(3)}(t,\tilde{z}^*) - i\big[H_s, Q_1^{(3)}(t,\tilde{z}^*)\big] \\ &\quad - \sum_{k=0}^{3}\sum_{l=\max\{0,k-1\}}^{\min\{k,2\}} \frac{C_l^k C_{2-l}^{3-k}}{C_1^3}\big[L^\dagger Q_{k-l}^{(k)}(t,\tilde{z}^*), Q_{1-k+l}^{(3-k)}(t,\tilde{z}^*)\big] - 4L^\dagger Q_2^{(4)}(t,\tilde{z}^*) \\ &= \frac{1}{3}\alpha(0)\big[L, Q_0^{(2)}(t,\tilde{z}^*)\big] + \frac{2}{3}z_t\big[L, Q_1^{(2)}(t,\tilde{z}^*)\big] - 2\gamma Q_1^{(3)}(t,\tilde{z}^*) - i\big[H_s, Q_1^{(3)}(t,\tilde{z}^*)\big] \\ &\quad - \big[L^\dagger Q_0^{(0)}(t,\tilde{z}^*), Q_1^{(3)}(t,\tilde{z}^*)\big] - \frac{1}{3}\big[L^\dagger Q_1^{(1)}(t,\tilde{z}^*), Q_0^{(2)}(t,\tilde{z}^*)\big] - \frac{2}{3}\big[L^\dagger Q_0^{(1)}(t,\tilde{z}^*), Q_1^{(2)}(t,\tilde{z}^*)\big] \\ &\quad - \frac{2}{3}\big[L^\dagger Q_1^{(2)}(t,\tilde{z}^*), Q_0^{(1)}(t,\tilde{z}^*)\big] - \frac{1}{3}\big[L^\dagger Q_0^{(2)}(t,\tilde{z}^*), Q_1^{(1)}(t,\tilde{z}^*)\big] - \big[L^\dagger Q_1^{(3)}(t,\tilde{z}^*), Q_0^{(0)}(t,\tilde{z}^*)\big] \\ &\quad - 4L^\dagger Q_2^{(4)}(t,\tilde{z}^*). \end{aligned} \tag{B6}$$

(6) When $n = 3, m = 2$,

$$\begin{aligned}\dot{Q}_2^{(3)}(t,\tilde{z}^*) &= \frac{2}{3}\alpha(0)\big[L, Q_1^{(2)}(t,\tilde{z}^*)\big] + \frac{1}{3}\tilde{z}_t^*\big[L, Q_2^{(2)}(t,\tilde{z}^*)\big] - 3\gamma Q_2^{(3)}(t,\tilde{z}^*) - i\big[H_s, Q_2^{(3)}(t,\tilde{z}^*)\big] \\ &\quad - \sum_{k=0}^{3}\sum_{l=\max\{0,k-2\}}^{\min\{k,1\}} \frac{C_l^k C_{1-l}^{3-k}}{C_2^3}\big[L^\dagger Q_{k-l}^{(k)}(t,\tilde{z}^*), Q_{2-k+l}^{(3-k)}(t,\tilde{z}^*)\big] - 4L^\dagger Q_3^{(4)}(t,\tilde{z}^*) \\ &= \frac{2}{3}\alpha(0)\big[L, Q_1^{(2)}(t,\tilde{z}^*)\big] + \frac{1}{3}\tilde{z}_t^*\big[L, Q_2^{(2)}(t,\tilde{z}^*)\big] - 3\gamma Q_2^{(3)}(t,\tilde{z}^*) - i\big[H_s, Q_2^{(3)}(t,\tilde{z}^*)\big] \\ &\quad - \big[L^\dagger Q_0^{(0)}(t,\tilde{z}^*), Q_2^{(3)}(t,\tilde{z}^*)\big] - \frac{2}{3}\big[L^\dagger Q_1^{(1)}(t,\tilde{z}^*), Q_1^{(2)}(t,\tilde{z}^*)\big] - \frac{1}{3}\big[L^\dagger Q_0^{(1)}(t,\tilde{z}^*), Q_2^{(2)}(t,\tilde{z}^*)\big] \\ &\quad - \frac{1}{3}\big[L^\dagger Q_2^{(2)}(t,\tilde{z}^*), Q_0^{(1)}(t,\tilde{z}^*)\big] - \frac{2}{3}\big[L^\dagger Q_1^{(2)}(t,\tilde{z}^*), Q_1^{(1)}(t,\tilde{z}^*)\big] - \big[L^\dagger Q_2^{(3)}(t,\tilde{z}^*), Q_0^{(0)}(t,\tilde{z}^*)\big] \\ &\quad - 4L^\dagger Q_3^{(4)}(t,\tilde{z}^*). \end{aligned} \tag{B7}$$

(7) When $n = m = 3$,

$$\begin{aligned}\dot{Q}_3^{(3)}(t,\tilde{z}^*) &= \alpha(0)\big[L, Q_2^{(2)}(t,\tilde{z}^*)\big] - 4\gamma Q_3^{(3)}(t,\tilde{z}^*) \\ &\quad - i\big[H_s, Q_3^{(3)}(t,\tilde{z}^*)\big] - \sum_{k=0}^{3}\sum_{l=\max\{0,k-3\}}^{\min\{k,0\}} \frac{C_l^k C_{0-l}^{3-k}}{C_3^3}\big[L^\dagger Q_{k-l}^{(k)}(t,\tilde{z}^*), Q_{3-k+l}^{(3-k)}(t,\tilde{z}^*)\big] - 4L^\dagger Q_4^{(4)}(t,\tilde{z}^*) \\ &= \alpha(0)\big[L, Q_2^{(2)}(t,\tilde{z}^*)\big] - 4\gamma Q_3^{(3)}(t,\tilde{z}^*) - i\big[H_s, Q_3^{(3)}(t,\tilde{z}^*)\big] - \big[L^\dagger Q_0^{(0)}(t,\tilde{z}^*), Q_3^{(3)}(t,\tilde{z}^*)\big] \\ &\quad - \big[L^\dagger Q_1^{(1)}(t,\tilde{z}^*), Q_2^{(2)}(t,\tilde{z}^*)\big] - \big[L^\dagger Q_2^{(2)}(t,\tilde{z}^*), Q_1^{(1)}(t,\tilde{z}^*)\big] - \big[L^\dagger Q_3^{(3)}(t,\tilde{z}^*), Q_0^{(0)}(t,\tilde{z}^*)\big] \\ &\quad - 4L^\dagger Q_4^{(4)}(t,\tilde{z}^*). \end{aligned} \tag{B8}$$

[1] M. O. Scully and M. S. Zubairy, *Quantum Optics* (Cambridge University Press, Cambridge, England, 1997).

[2] A. J. Leggett, S. Chakravarty, A. T. Dorsey, M. P. A. Fisher, A. Garg, and W. Zwerger, Rev. Mod. Phys. **59**, 1 (1987).

[3] M. A. Nielsen and I. L. Chuang, *Quantum Computation and Quantum Information* (Cambridge University Press, Cambridge, England, 2000).
[4] S. John and J. Wang, Phys. Rev. Lett. **64**, 2418 (1990); S. John and T. Quang, Phys. Rev. A **52**, 4083 (1995); O. Toader, T. Y. M. Chan, and S. John, Phys. Rev. Lett. **92**, 043905 (2004).
[5] C. Emary and T. Brandes, Phys. Rev. Lett. **90**, 044101 (2003).
[6] S. De Liberato, C. Ciuti, and I. Carusotto, Phys. Rev. Lett. **98**, 103602 (2007).
[7] J. Li *et al.*, Nat. Commun. **4**, 1420 (2013).
[8] A. G. Kofman and G. Kurizki, Phys. Rev. Lett. **93**, 130406 (2004).
[9] H. Zheng, S. Y. Zhu, and M. S. Zubairy, Phys. Rev. Lett. **101**, 200404 (2008).
[10] X. Cao, J. Q. You, H. Zheng, A. G. Kofman, and F. Nori, Phys. Rev. A **82**, 022119 (2010).
[11] S. Agarwal, S. M. Hashemi Rafsanjani, and J. H. Eberly, Phys. Rev. A **85**, 043815 (2012).
[12] A. T. Sornborger, A. N. Cleland, and M. R. Geller, Phys. Rev. A **70**, 052315 (2004).
[13] T. Werlang, A. V. Dodonov, E. I. Duzzioni, and C. J. Villas-Bôas, Phys. Rev. A **78**, 053805 (2008).
[14] B. L. Hu, J. P. Paz, and Y. Zhang, Phys. Rev. D **45**, 2843 (1992).
[15] L. Diósi, N. Gisin, and W. T. Strunz, Phys. Rev. A **58**, 1699 (1998); W. T. Strunz, L. Diósi, and N. Gisin, Phys. Rev. Lett. **82**, 1801 (1999).
[16] T. Yu, L. Diósi, N. Gisin, and W. T. Strunz, Phys. Rev. A **60**, 91 (1999).
[17] W. T. Strunz and T. Yu, Phys. Rev. A **69**, 052115 (2004).
[18] J. Jing and T. Yu, Phys. Rev. Lett. **105**, 240403 (2010).
[19] J. Jing, X. Zhao, J. Q. You, W. T. Strunz, and T. Yu, Phys. Rev. A **88**, 052122 (2013).
[20] D. Lacroix, Phys. Rev. E **77**, 041126 (2008).
[21] G. Clos and H. P. Breuer, Phys. Rev. A **86**, 012115 (2012).
[22] H. Mäkelä and M. Möttönen, Phys. Rev. A **88**, 052111 (2013).
[23] B. Peropadre, D. Zueco, D. Porras, and J. J. García-Ripoll, Phys. Rev. Lett. **111**, 243602 (2013).
[24] P. Forn-Díaz, J. Lisenfeld, D. Marcos, J. J. García-Ripoll, E. Solano, C. J. P. M. Harmans, and J. E. Mooij, Phys. Rev. Lett. **105**, 237001 (2010).
[25] T. Yu, Phys. Rev. A **69**, 062107 (2004).
[26] J. Jing, X. Zhao, J. Q. You, and T. Yu, Phys. Rev. A **85**, 042106 (2012).
[27] I. de Vega, D. Alonso, and P. Gaspard, Phys. Rev. A **71**, 023812 (2005).
[28] J. Roden, A. Eisfeld, W. Wolff, and W. T. Strunz, Phys. Rev. Lett. **103**, 058301 (2009).
[29] D. Süß, A. Eisfeld, and W. T. Strunz, arXiv:1402.4647.